# Supporting Information:

# High Stable Zinc Metal Anode Enabled by Oxygen Functional Groups for Advanced Zn-ion Supercapacitors

*Kangyu Zou,[a] Peng Cai,[a] Xinglan Deng,[a] Baowei Wang,[a] Cheng Liu,[a] Zheng Luo,[a] Xiaoming Lou,[c] Hongshuai Hou,[a] Guoqiang Zou,*[a] and Xiaobo Ji[a, b]*

*[a]College of Chemistry and Chemical Engineering, Central South University, Changsha, 410083, China*

*[b]School of Metallurgy and Chemical Engineering, JiangXi University of Science and Technology, 86 Hongqi Road, Ganzhou 341000, China*

*[c]School of Materials and Chemistry Engineering, Hunan Institute of Technology, 18 Henghua Rd. Hengyang, China*

23 Feb 2021
Note added since first publication:
This Supplementary Information replaces that originally published on 10 Dec 2020, in which there was an incorrect structure for konjac glucomannan (KGM) in Fig. S12. The correct structure is shown in this updated version.

**Corresponding Author**

* Email address: gq-zou@csu.edu.cn;

Tel: +86 731-88877237; Fax: +86 731- 88879616.

## Experimental Section

### Preparation of Zn@KGM Anode

The bare Zn foil was polished by using abrasive paper for removing surface passivation layer. The KGM powder (1g) was dissolved in 50 mL deionized water to obtain a homogeneous solution at 80 °C and kept at 80 °C for 15 minutes. Then, the 0.2 g $Na_2CO_3$ powder was dissolved in another 5 mL deionized water. Subsequently, the later solution was quickly added to the former solution and resulting solution began to gelatinous. After stirring intensely for 2 minutes, formed KGM gel was homogeneously coated on the fresh Zn foil, which was further freeze-dried to prepare Zn@KGM anode.

### Materials characterization

The structures of the obtained specimens were analyzed by X-ray diffractometer (XRD, Rigaku) with a Cu-Ka radiation of 0.15418 nm (V=30 kV, I = 25 mA). The scanning electron microscopy (SEM, Hitachi S-4800) was carried out to evaluate the surface morphologies of bare Zn and Zn@KGM anodes before and after Zn striping/plating. The detailed compositions were determined by using an X-ray photoelectron spectroscopy analyzer (XPS) (VG Multi Lab 2000 system) and Fourier transform infrared spectrometer (FTIR) (Bruker Equinox 55 spectrometer). Wetting angles of 5 μL water droplets on the bare Zn and Zn@KGM anodes were measured with a Dataphysics OCA20 contact angle meter at ambient atmosphere.

### Electrochemical measurements

Activated carbon (AC) cathodes were acquired by mixing 80 wt% active materials, 10 wt% binder polyvinylidene fluoride (PVDF), and 10 wt% conductive carbon (Super P) dissolved in N-methyl pyrrolidinone (NMP). Then, the resulting slurries were coated on a stainless-steel foil and the as-prepared electrodes were dried under vacuum at 80 °C for 10 h. The bare Zn and Zn@KGM foils were first cut into disc-shaped electrodes. Symmetric batteries were directly used two pieces of bare Zn and Zn@KGM foils as electrodes. The electrochemical performance of AC electrodes was

characterized by employing a two-electrode system with bare Zn and Zn@KGM as counter electrode. The electrolyte is 2 M $ZnSO_4$ solution without any additives throughout the whole work while the separator is a Whatman GF/C glass fiber membrane. All the electrochemical measurements were carried out at room temperature.

For symmetric batteries, galvanostatic charging-discharging (GCD) cycling at a current density of 0.2-2.0 mA $cm^{-2}$ and a total capacity of 0.2-2.0 mA $cm^{-2}$ was on a LANDCT2001A battery-testing instrument. Tafel plots were recorded in three-electrode system with an Ag/AgCl and a platinum foil as reference and counter electrodes, respectively. Electrochemical impedance spectra (EIS) were measured by a MULTI AUTOLAB M204 (MAC90086)

For Zn-ion supercapacitors (ZICs) with the AC cathode, cyclic voltammetry (CV) curves with different scan rates and EIS were measured by a MULTI AUTOLAB M204 (MAC90086). Galvanostatic charge/discharge (GCD) surveys were collected on an Arbin BT2000 instrument at different current densities within an appropriate voltage window. Cycle-life tests were recorded on a Land CT2001A model battery system.

The specific capacitance (C, F $g^{-1}$), energy density (E, W h $kg^{-1}$), and power density (P, W $kg^{-1}$) of ZICs, based on the GCD measurements, can be calculated according to the following equations.

$$C = It/\Delta Vm \qquad eqn\ (\mathbf{1})$$

$$E = C(V_{max}^2 - V_{min}^2)/2 \times 3.6 \qquad eqn\ (\mathbf{2})$$

$$P = E \times 3600/t \qquad eqn\ (\mathbf{3})$$

Where $I$ (A) represents the discharge current, t (s) represents the discharge time, $V_{max}$ (V) and $V_{min}$ (V) are the initial and final discharge potentials, $\Delta V$ (V) is the potential change, and $m$ (g) is the total mass of active material.

## Supplementary Figures

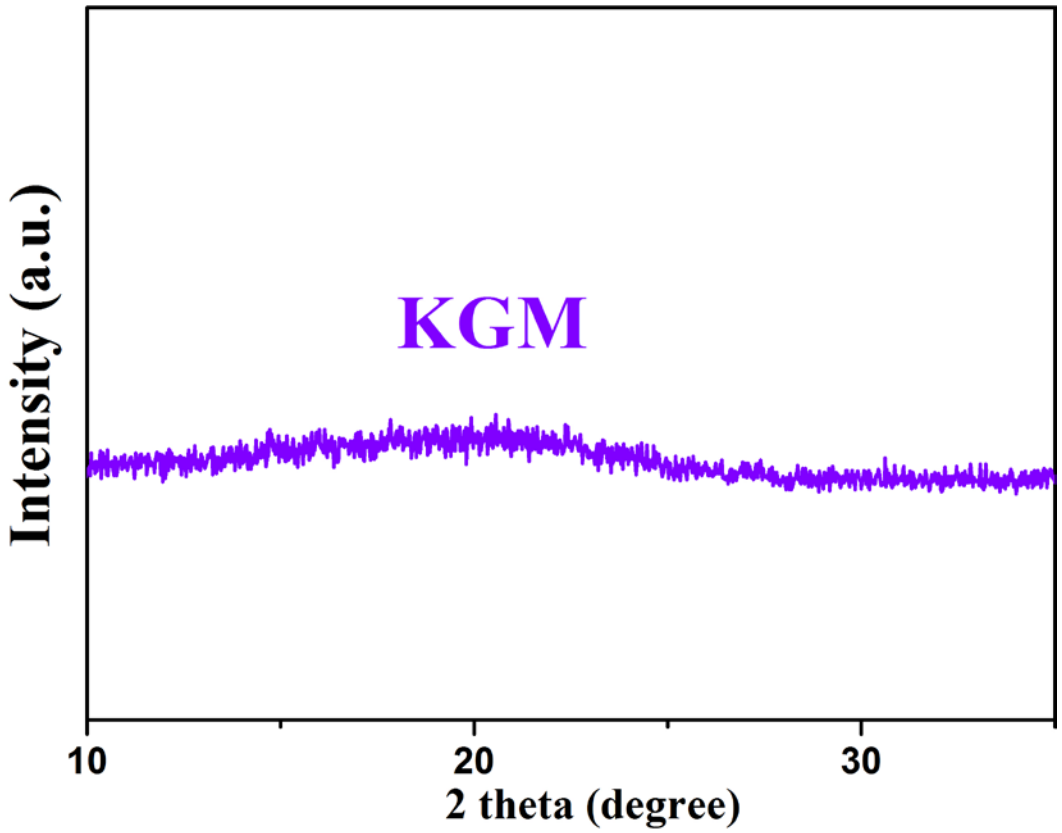


**Figure S1** The XRD patterns of Zn@KGM anodes in the selected range.

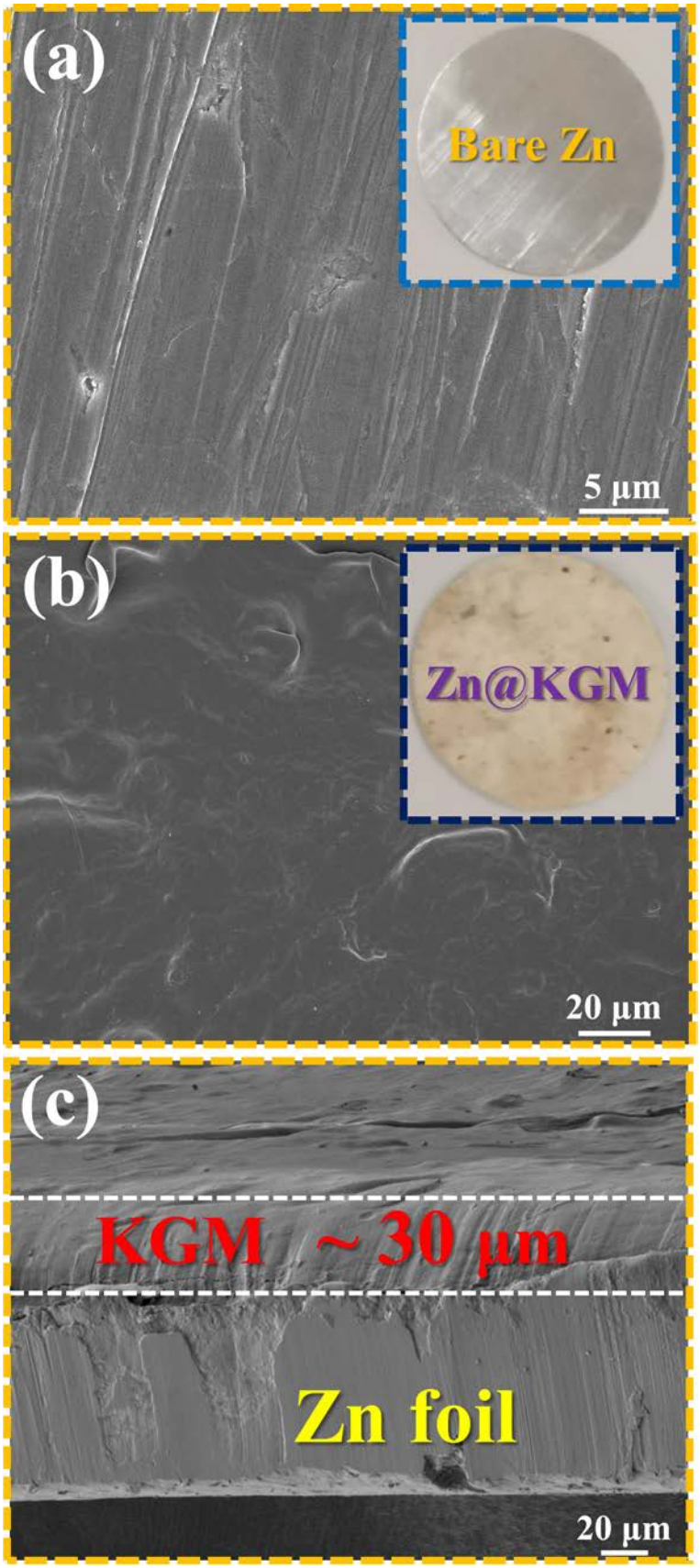


**Figure S2** SEM images of (a) bare Zn and (b) Zn@KGM with the insets of optical photographs. (c) Cross-section SEM image of Zn@KGM.

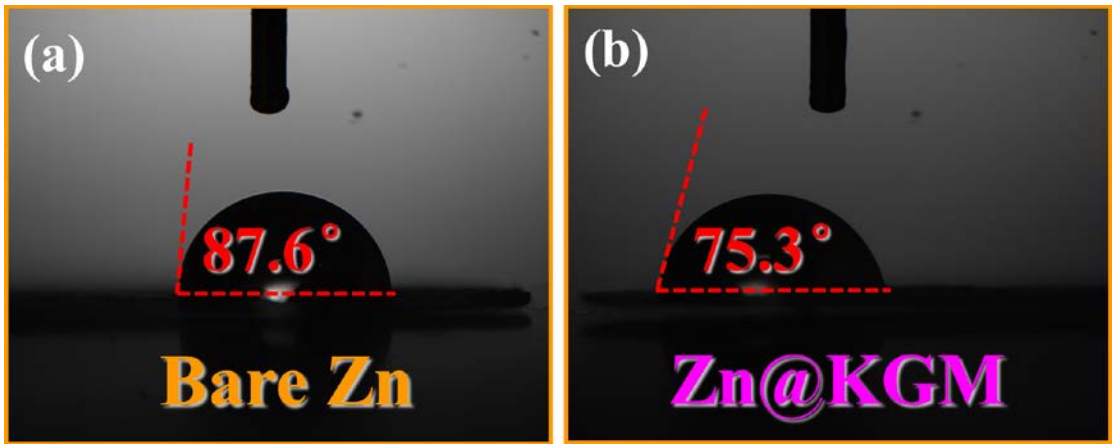


**Figure S3** Contact angle measurements of (**a**) bare Zn and (**b**) Zn@KGM anodes.

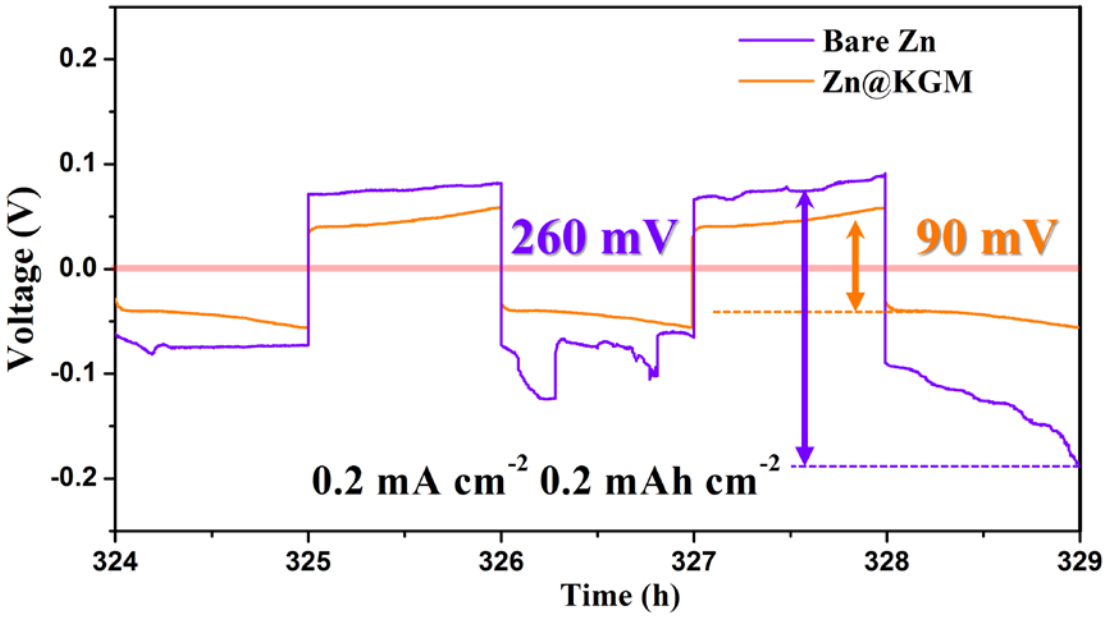


**Figure S4** Detailed voltage profiles of bare Zn and Zn@KGM symmetric cells at specific cycling times of 324-329 h at 0.2 mA $cm^{-2}$ for 0.2 mAh $cm^{-2}$.

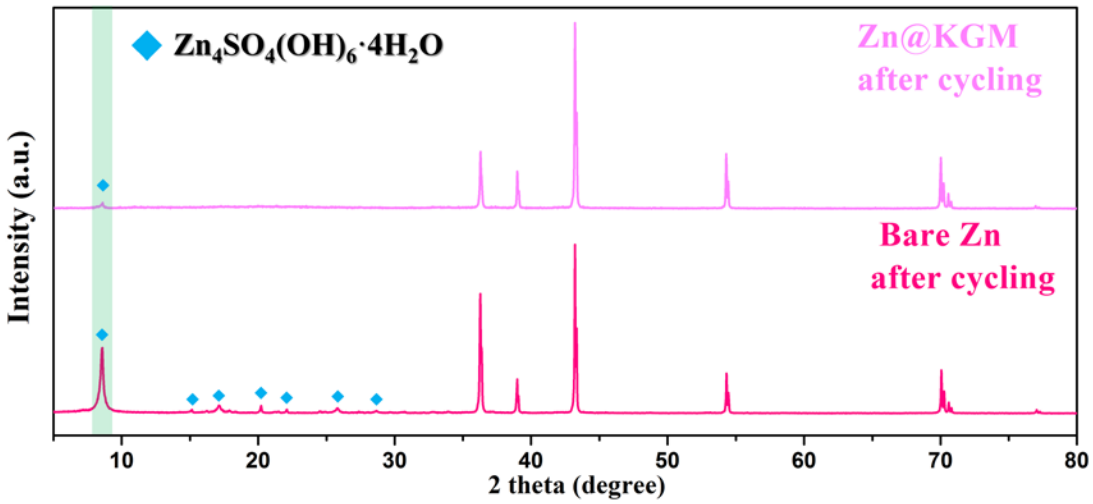


**Figure S5** XRD patterns of bare Zn and Zn@KGM anodes after cycling in symmetric cells.

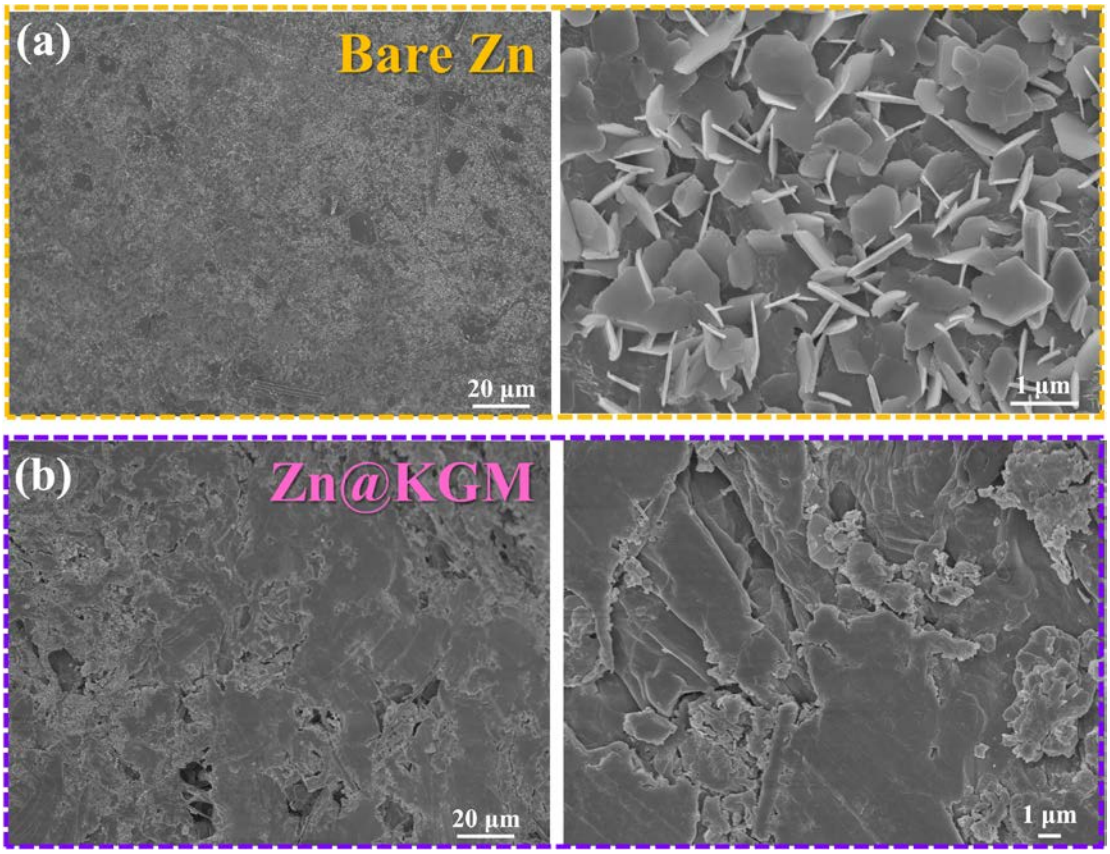


**Figure S6** SEM images of (**a**) bare Zn and (**b**) Zn@KGM anodes in symmetric cells after the first plating process at 0.2 mA $cm^{-2}$ for 0.2 mAh $cm^{-2}$.

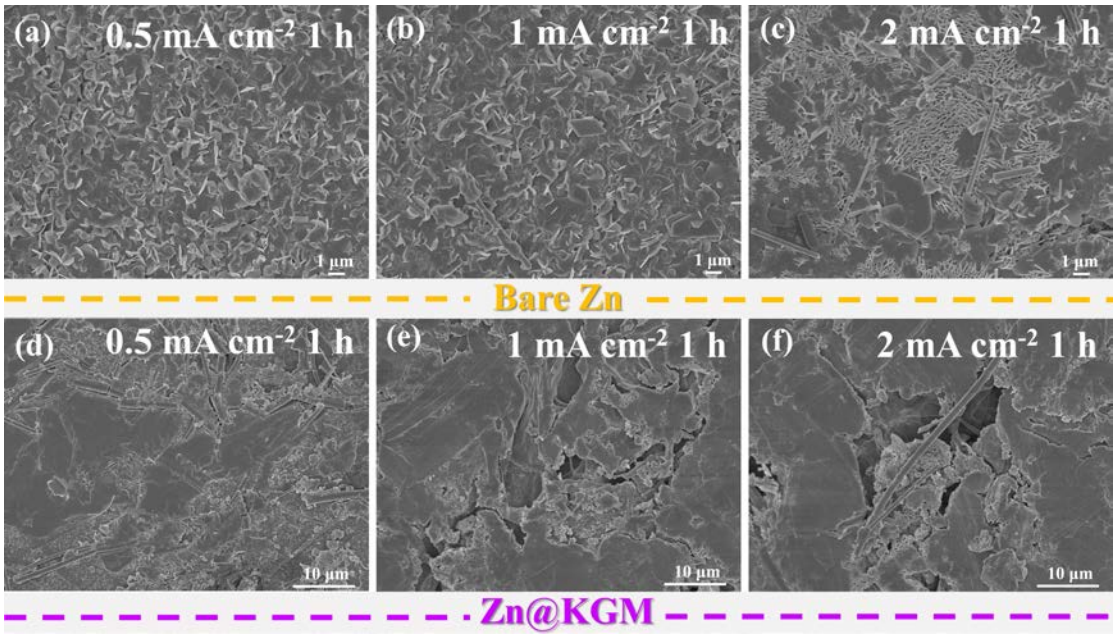


**Figure S7** SEM images of (**a-c**) bare Zn and (**d-f**) Zn@KGM anodes in symmetric cells after the first plating at different current densities for 1h.

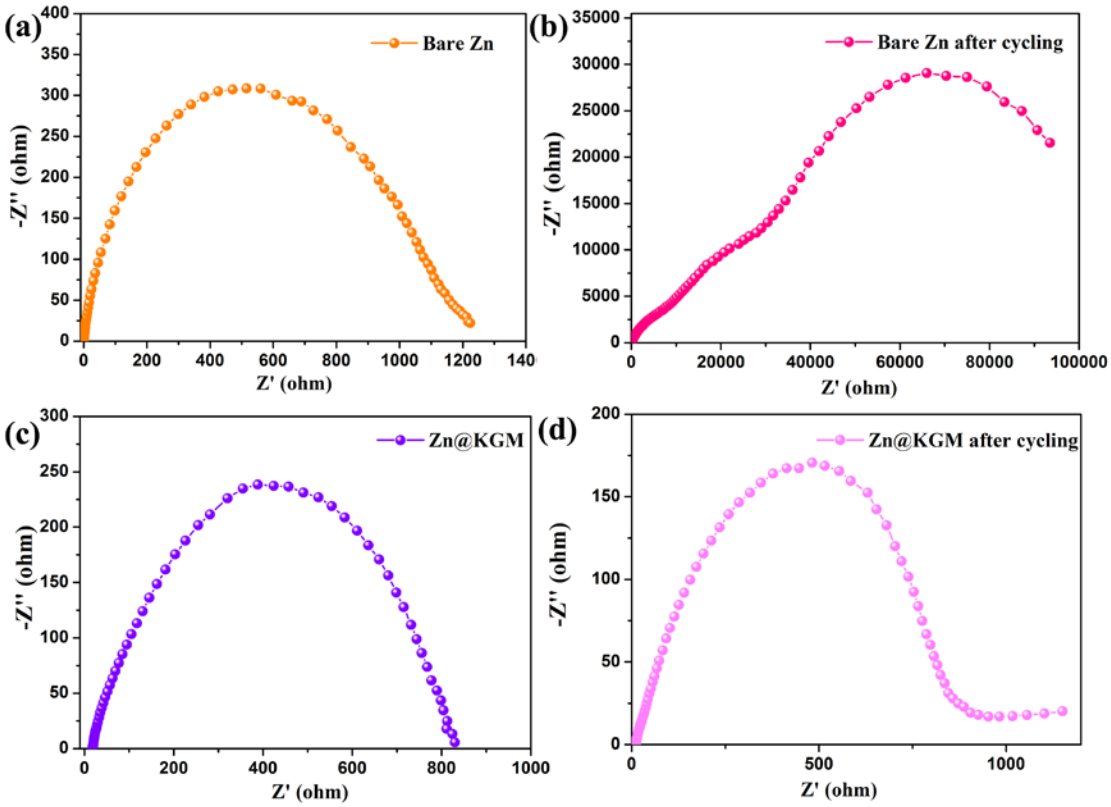


**Figure S8** Nyquist plots of (**a**, **b**) bare Zn and (**c**, **d**) Zn@KGM anodes before and after cycling in symmetric cells.

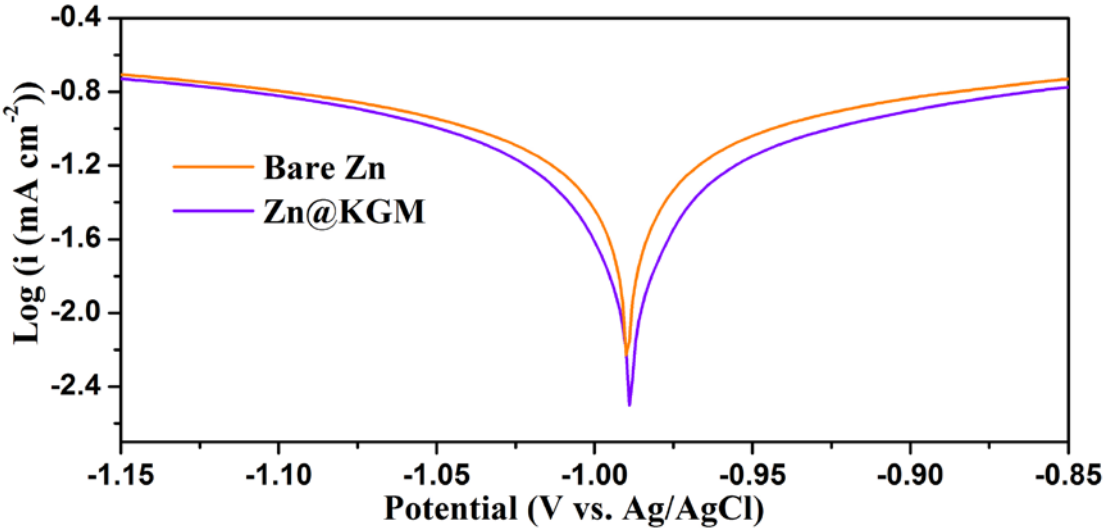


**Figure S9** Tafel plots of corrosion behaviors for bare Zn and Zn@KGM anodes.

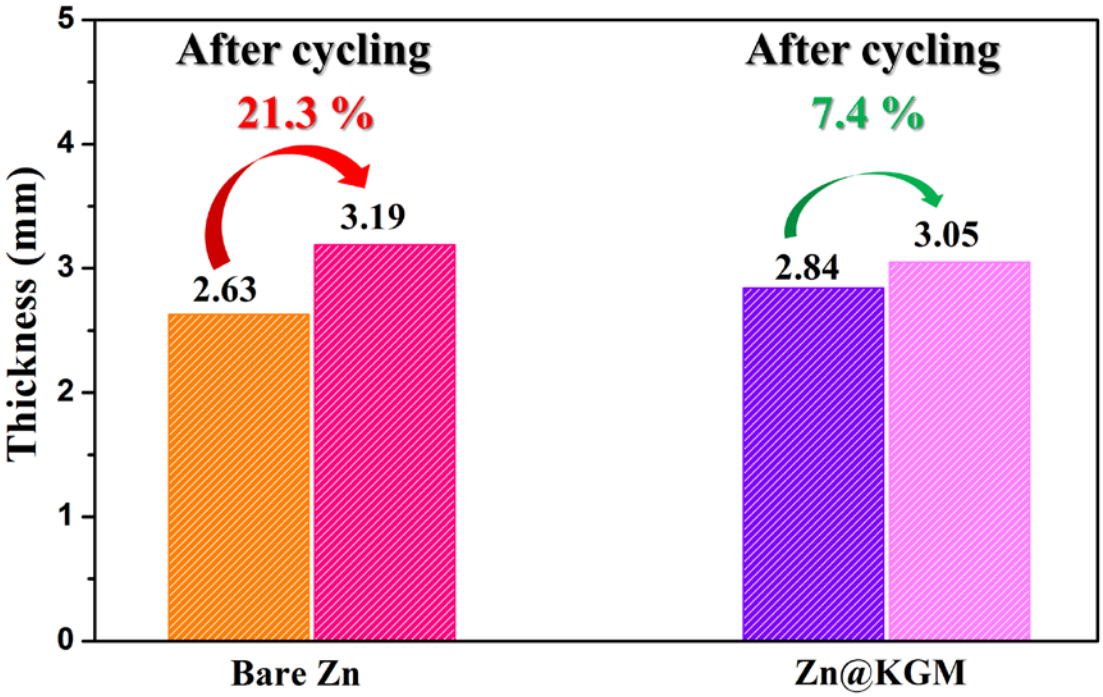


**Figure S10** Thickness change of the bare Zn and Zn@KGM symmetric cells before and after cycling at 0.2 mA $cm^{-2}$.

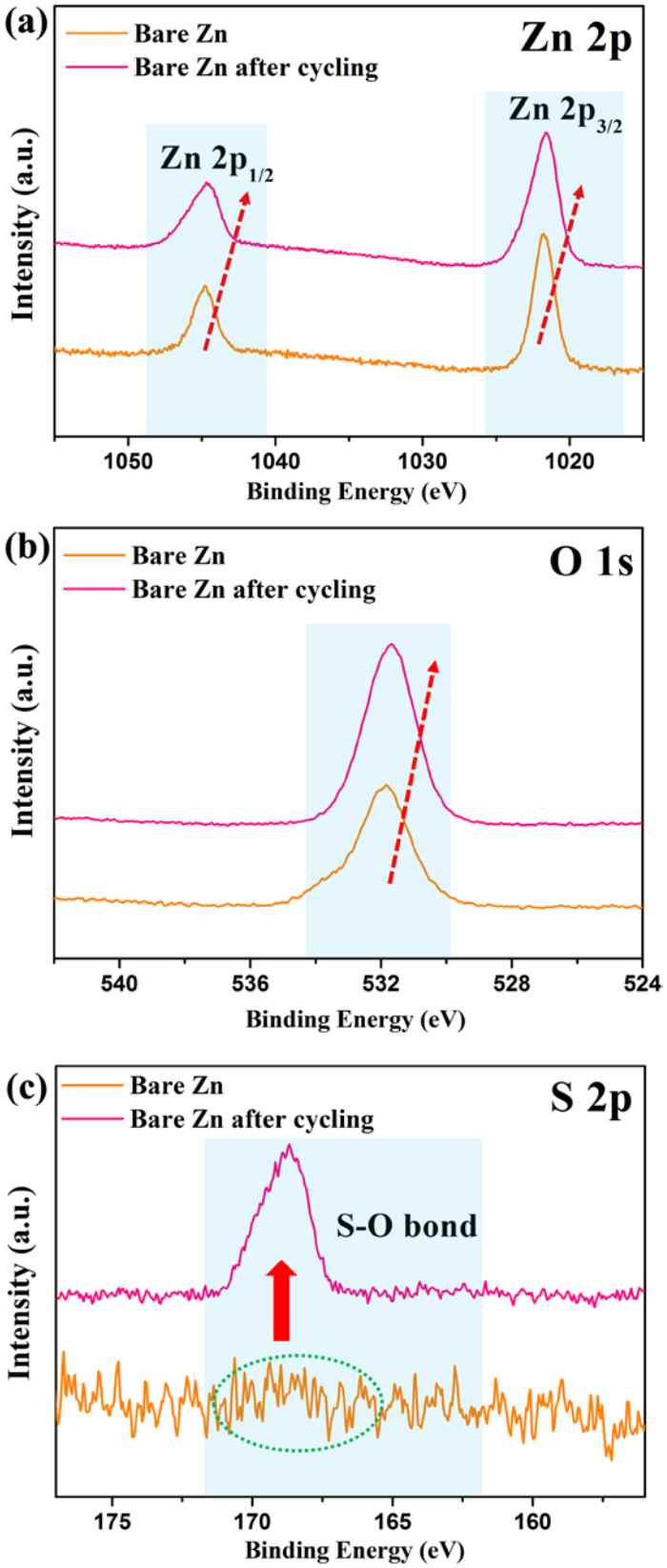


**Figure S11** High-resolution (**a**) Zn 2p spectra, (**b**) O 1s spectra and (**c**) S 2p spectra of bare Zn anodes before and after cycling in symmetric cells.

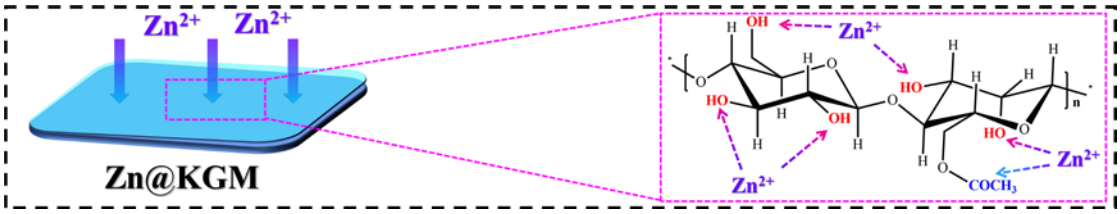


**Figure S12** Possible mechanism for stabilized Zn anode triggered by rich oxygen functional groups.

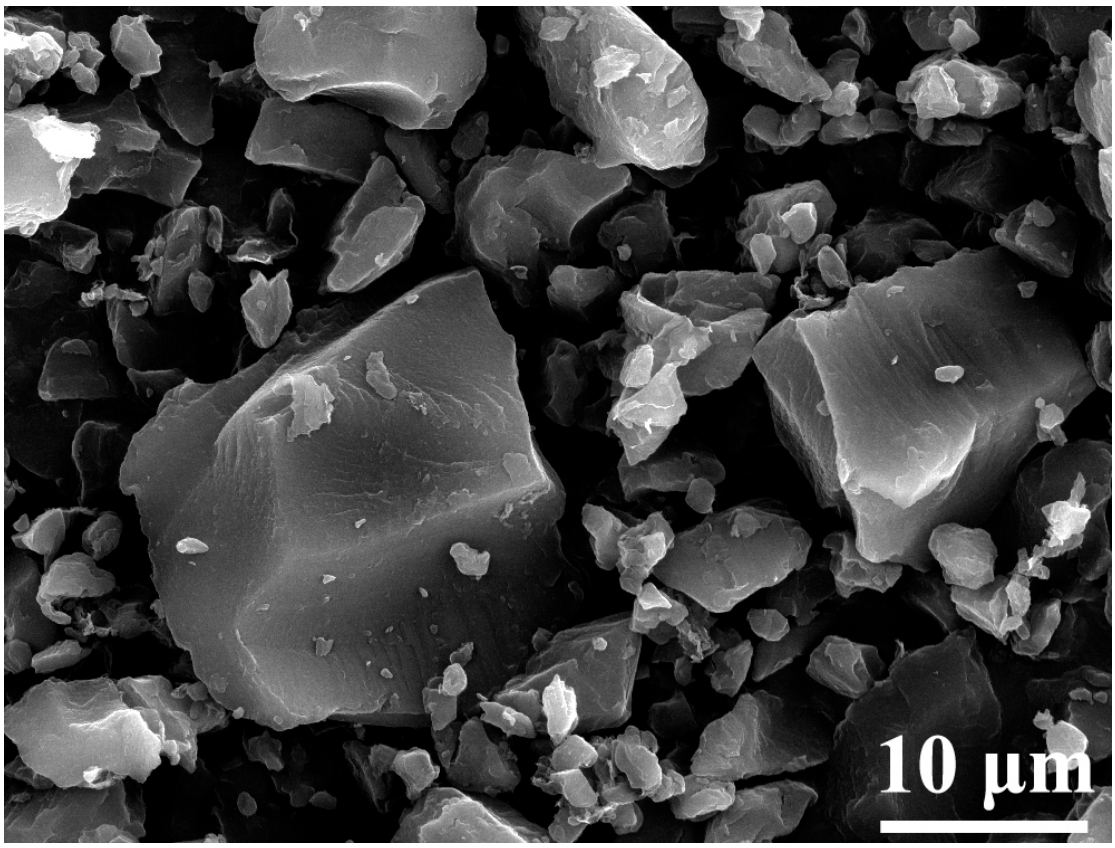


**Figure S13** SEM images of AC.

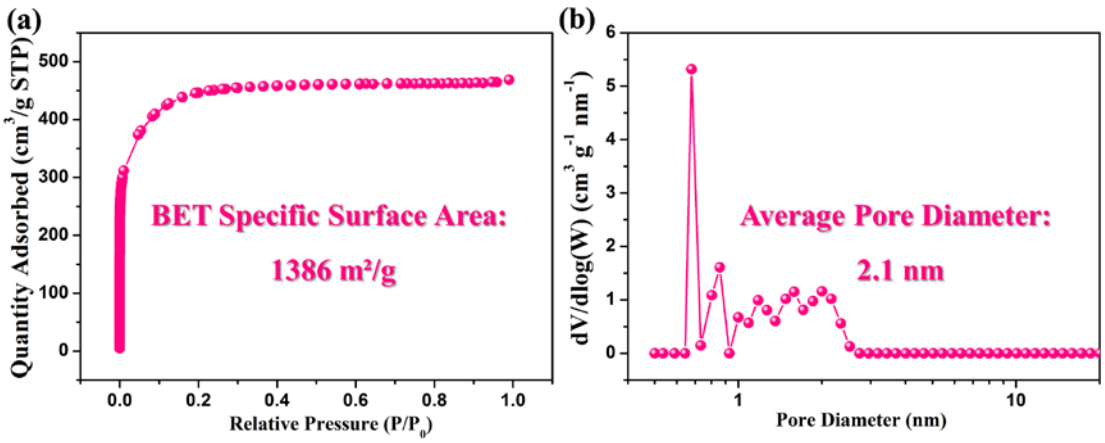


**Figure S14** (**a**) $N_2$ adsorption-desorption isotherms and (b) pore size distributions of AC.

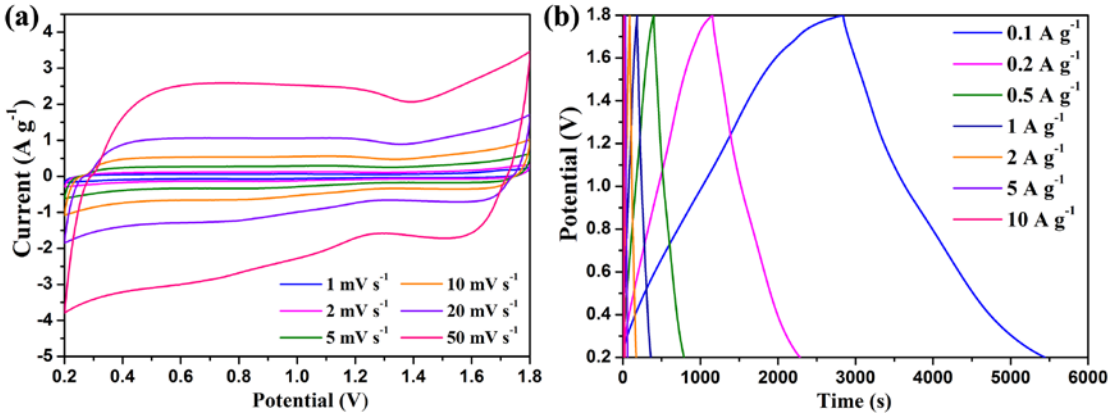


**Figure S15** (**a**) CV curves and (**b**) GCD profiles of Zn//AC ZIC.

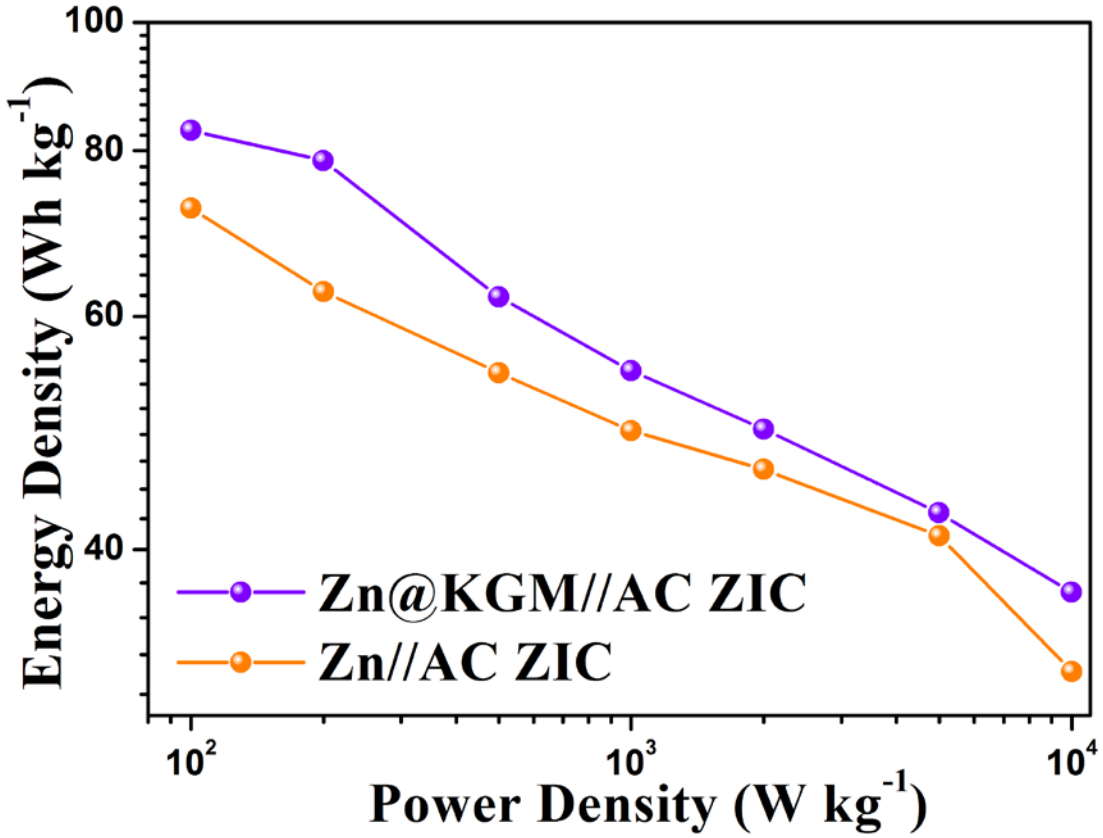


**Figure S16** Ragone plot of Zn//AC and Zn@KGM//AC ZICs.

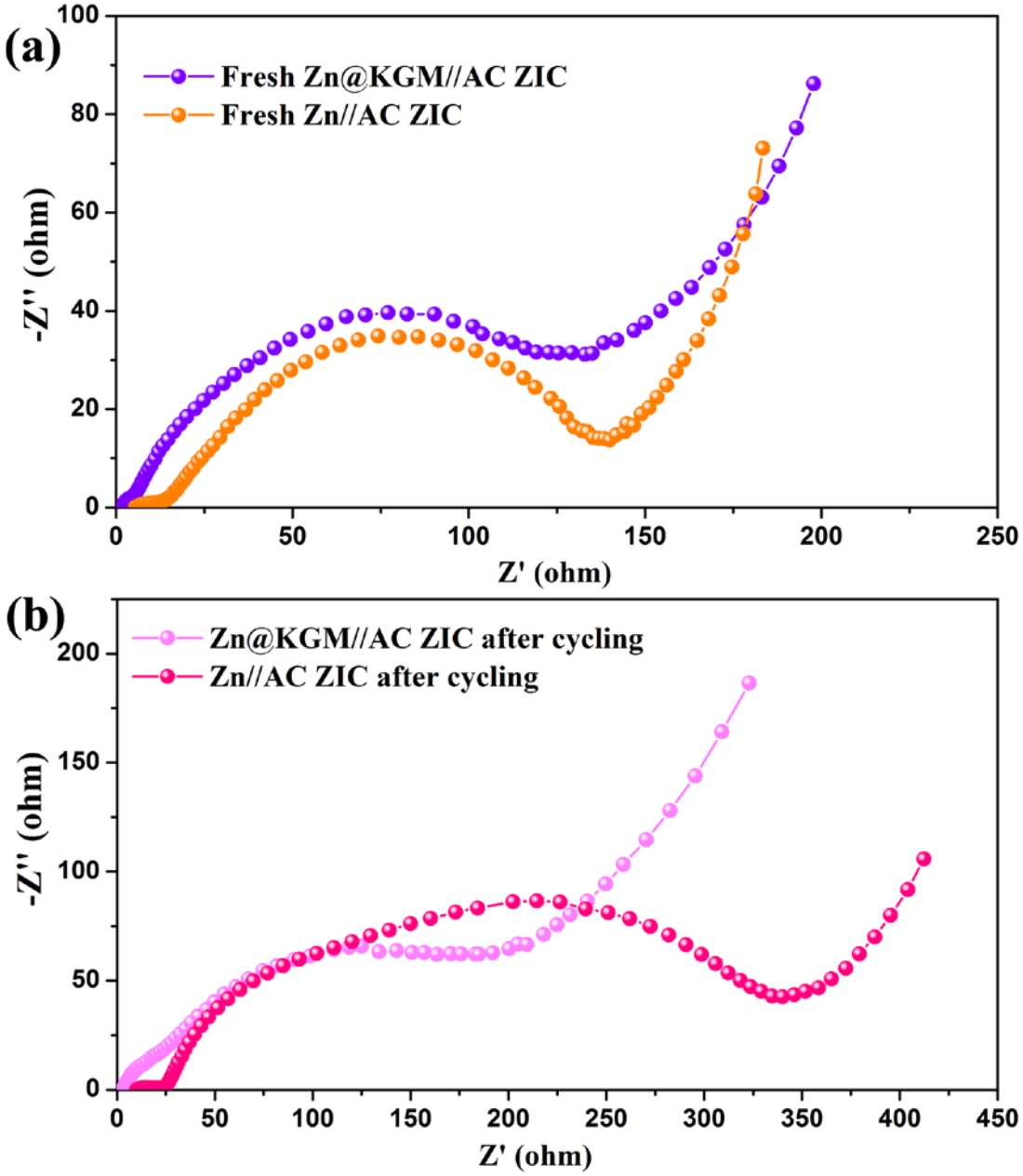


**Figure S17** Nyquist plots of (**a**) Zn//AC and (**b**) Zn@KGM//AC ZICs before and after cycling.

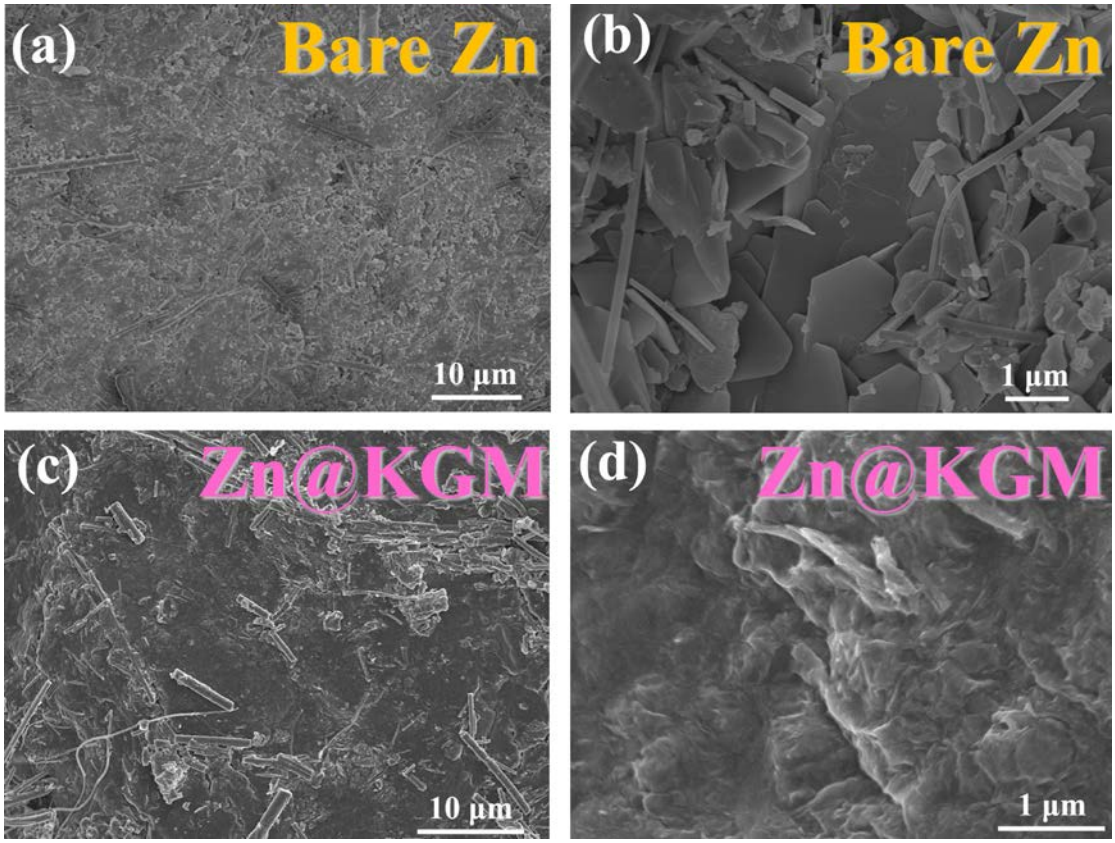


**Figure S18** SEM images of (**d**, **e**) bare Zn and (**f**, **g**) Zn@KGM anodes in ZICs after 100 cycles at 1 A $g^{-1}$.

**Table S1**. The fitting $R_{ct}$ values of bare Zn and Zn@KGM anodes before and after cycling in symmetric cells.

| **Sample** | **$R_{ct}$** |
|---|---|
| Bare Zn anode before cycling | 1150 |
| Zn@KGM anode before cycling | ~10000 |
| Bare Zn anode after cycling | 750 |
| Zn@KGM anode after cycling | 850 |

**Table S2**. The fitting $R_{ct}$ values of Zn//AC and Zn@KGM//AC ZICs before and after cycling.

| **Sample** | **$R_{ct}$** |
|---|---|
| Zn//AC ZIC before cycling | 140 |
| Zn@KGM//AC ZIC before cycling | 130 |
| Zn//AC ZIC after cycling | 330 |
| Zn@KGM//AC ZIC after cycling | 250 |